Proceedings of Meetings on Acoustics

JANUARY 03 2025

Harnessing the potential of a silent mesopelagic observation system integrated with active acoustics for mesopelagic faunal studies FREE

Rendhy Moreno Sapiie; Lauren Freeman; Christopher Roman; David Casagrande; Brennan Phillips

Proc. Mtgs. Acoust. 54, 005001 (2024)
https://doi.org/10.1121/2.0001988

Volume 54 http://acousticalsociety.org/

Acoustics Week in Canada
Joint Meeting
186th Meeting of the Acoustical Society of America
and the Canadian Acoustical Association

Ottawa, Ontario, Canada
13-17 May 2024

Acoustical Oceanography: Paper 3aAOb3

Harnessing the potential of a silent mesopelagic observation system integrated with active acoustics for mesopelagic faunal studies

Rendhy Moreno Sapiie
Department of Ocean Engineering, University of Rhode Island, Narragansett, RI, 02881; rendhymoreno27@gmail.com

Lauren Freeman
Naval Undersea Warfare Center Newport Division, Newport, RI, 02841; lauren.a.freeman3.civ@us.navy.mil

Christopher Roman and David Casagrande
Graduate School of Oceanography, University of Rhode Island, Narragansett, RI, 02882; croman2@uri.edu; davecasa@gmail.com

Brennan Phillips
Department of Ocean Engineering, University of Rhode Island, Narragansett, RI, 02882; brennanphillips@uri.edu

Over the past six decades, extensive research has explored how marine animals interact with oceanographic sampling equipment, highlighting the impact of light and sound emissions on fauna behavior during surveys. Anthropogenic disturbances—such as sound, light, and hydrodynamic forces—affect quantitative observations in the twilight zone, but the underlying mechanisms remain unclear. To investigate, we developed a "silent" tethered mesopelagic observation system for depths up to 1000 m. It integrates multi-frequency echosounders, dimmable lights, and a sensitive low-light camera to track animal behavior at various spatiotemporal scales. Exclusively battery-powered, the system minimizes acoustic output in the water by eliminating the need for noisy ship engines. In July 2023, we conducted its first test dive in Bermuda, while opportunistically documenting mesopelagic fauna responses to ~5-minute interval light changes during a new moon phase. Assimilation of multiple perspective echosounder data at 38-kHz revealed a weak positive correlation (R = 0.2657) between swimming direction and distance from the system for detected animals within 20 meters. Animals closer to the system (0–10 m) were more likely to swim towards it, while those farther away (10–20 m) swam in the opposite direction, regardless of light presence. These findings underscore the need for more comprehensive future experiments.

Published by the Acoustical Society of America

 https://doi.org/10.1121/2.0001988

1. INTRODUCTION

There is a significant gap in our understanding on the effects of disturbance caused by oceanographic sampling tools that could potentially bias our observations of underwater animals during surveys.[1,2] Many studies have postulated that most epipelagic and mesopelagic animals rely on visual cues in their environment[3] and light stimuli produced from oceanographic equipment has strong perturbing effects on certain animal species during observations using active acoustic methods.[4–6] The effects of artificial light on epipelagic and mesopelagic animals have been further explored in several studies that utilized custom-designed, tethered instrument platforms. These platforms were low-profile, lacked sound sources, and were equipped with artificial lighting that operated at various colors or wavelengths (e.g.[5–7]). Most studies have suggested that white light had a perturbing effect on certain faunal species and red light was less obtrusive due to the rapid attenuation of this wavelength.[5,6,8] A recent in situ experiment using a similar instrument platform found that animals were affected by artificial light in various colors, including red light, which contradicts previous findings.[7] However, many of these studies were conducted on large research vessels, which are significant sound sources and have evidently elicited downward swimming behavior patterns from near surface and epipelagic animals.[9–11] Thus, the potential effects of sound in previous studies cannot be overlooked.

To this end, we developed a custom mesopelagic observation system designed for minimally intrusive midwater observations, allowing the study of animal behavior in their natural environment with minimal light and acoustic output. This is achieved by operating independently of ship power, enabling the ship's generators to be shut off. These efforts are the result of a multi-year study in partnership with Naval Undersea Warfare Center Division Newport (NUWCDIVNPT). In 2023, we conducted full-scale testing of the this unobtrusive system in Bermuda, and this manuscript presents our initial findings from these experiments.

2. EXPERIMENT SETUP

A. SYSTEM OVERVIEW

The system was installed aboard the 41-foot research vessel, the R/V Henry Stommel, operated by the Bermuda Institute of Ocean Sciences (BIOS) and was comprised of two main components: the payload and the winch system (Figure 1a,b,c). The custom-designed active heave compensation winch, featuring a 0.25" (6 mm) diameter fiber optic cable with three fiber optic single-mode passes, tethered to a battery-powered payload instrument frame with a fiber optic multiplexer, allows for instant payload control and real-time data visualization. The heave compensation feature facilitates smooth and consistent depth control even in variable sea-state conditions without the use of underwater thrusters. The winch tether has no power conductors hence reducing the overall scale of the system as well as cable drag in the water column. Each component of this system was powered by an isolated direct current (DC) power supply and independent from ship power, which allows operations to be conducted with full boat engine/generator shutdown and a reduced risk of electrical noise interference with the acoustical payload. The winch has been modified to run on 600 Volts DC (VDC) from a custom battery array, while the payload system was powered through a 24 VDC battery pack housed in a titanium bottle. All topside equipment was powered using either a portable AC/DC power supply or by tapping into the 220 Volts Alternating Current (VAC) power from the winch. This unique setup permits midwater exploration without noise contribution from the boat engines and generators, which has not been explored in previous studies that utilize similar systems.[5–7]

The payload module consisted of a modular aluminum instrument frame populated with a battery pack, telemetry bottle, and configurable sensor options (Figure 1(d)). The sensors used were a high-definition/low-light sensitive camera (Canon ME20F-SH) used in a different study by Gruber et al.,[12] two dimmable Deep-Sea Power & Light LED SeaLites (10,000 lm maximum output, dimmable to ∼140 lm at minimum output), a self-contained StarOddi mini conductivity-temperature-depth (CTD) logger with compass (DST Mag-

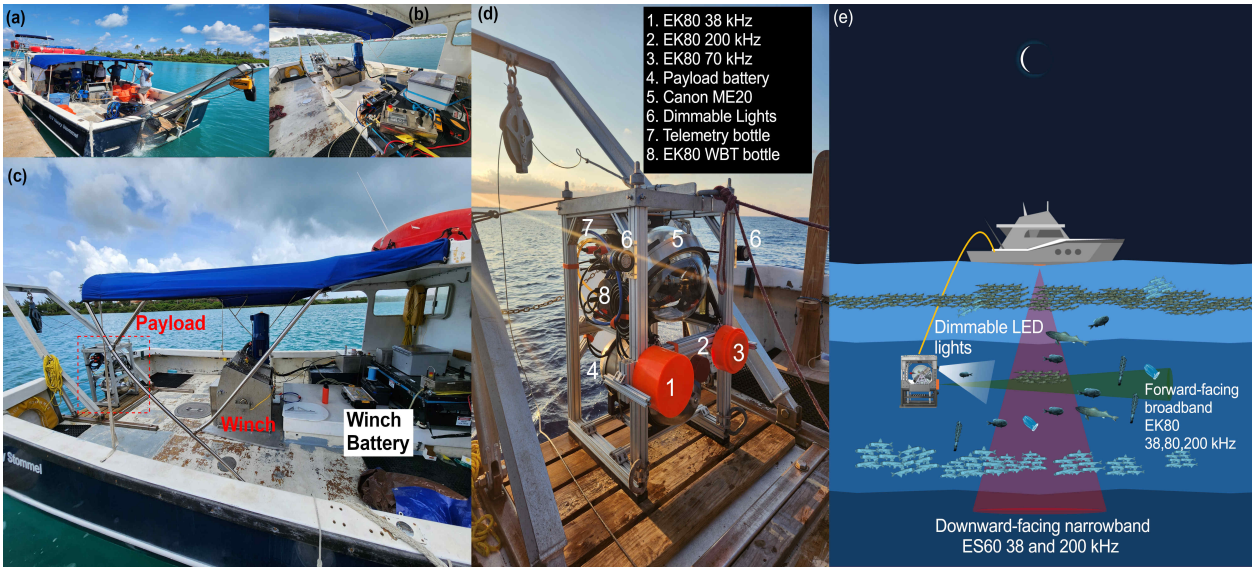

Figure 1: The mesopelagic observer system setup and operation scheme. (a) An overview of the work deck of the 41-foot operating vessel The R/V Stommel. (b) The winch, controller, and winch battery. (c) Side view of the workspace highlighting components of the system. A ship mounted Simrad ES60 downward echosounder was installed on the starboard side of boat (not shown). (d) The subsea payload with major components identified. (e) An overview of how the system works during operations. Dives were conducted post-sundown during the new moon phase.

netic), and a broadband forward-facing Simrad EK80 system. The custom EK80 system, consisting of two repackaged wideband transceivers (WBT) and three split-beam transducers operating at 38, 70, and 200 kHz (ES38-18DK, ES70-18CD, ES200-7DK), has been used in previous studies, with modifications such as the addition of a power filter to reduce electrical noise.[13,14]

B. OPERATION

The system integrated multiple hydro-acoustic sensors and video observations to study midwater fauna distribution and their behavioral responses to artificial light emitted in front of the payload across different temporal and spatial scales (Figure 1(e)). The ship-mounted dual-frequency single-beam Simrad ES60 echosounder with the Simrad 30/200 combi transducer (termed ES60) provided a 'bird's-eye view' of the water column from above, detecting sound scattering layers (SSL) and large-scale swimming patterns. The forward-facing EK80 broadband multifrequency echosounder (termed EK80) tracked single animal targets at high resolution and resolved their swimming patterns up to 100 m, while the low-light imaging platform achieved a higher taxonomic resolution of animal assemblages within a limited range (<10 m).

The system was deployed approximately 10 km off the eastern coast of Bermuda (GMT-3) in water depths of around 1200-1500 m from July 12-21, 2023 (Figure 2). The dives were conducted at sunset during the new moon phase, based on the hypothesis that animals are more sensitive to light during this time, causing SSLs to stay at shallower depths. Dive operations proceeded as follows: All sensors were synchronized to UTC time. The ES60 echosounder initially identified SSLs in the water column. Once a target SSL was confirmed, the payload was lowered to the corresponding depth while continuously collecting hydro-acoustic and imaging data. At a stable SSL (i.e., where the layer remains constant), the payload's artificial lights were turned on to maximum intensity and then switched off over approximately 5-minute intervals to observe faunal responses to changes in light. This setup allows for documenting changes in animal assemblages and distributions at different time and spatial scales. This final product is a result of data assimilation from multiple vantage points —both above and in front of the payload— providing a unique perspective

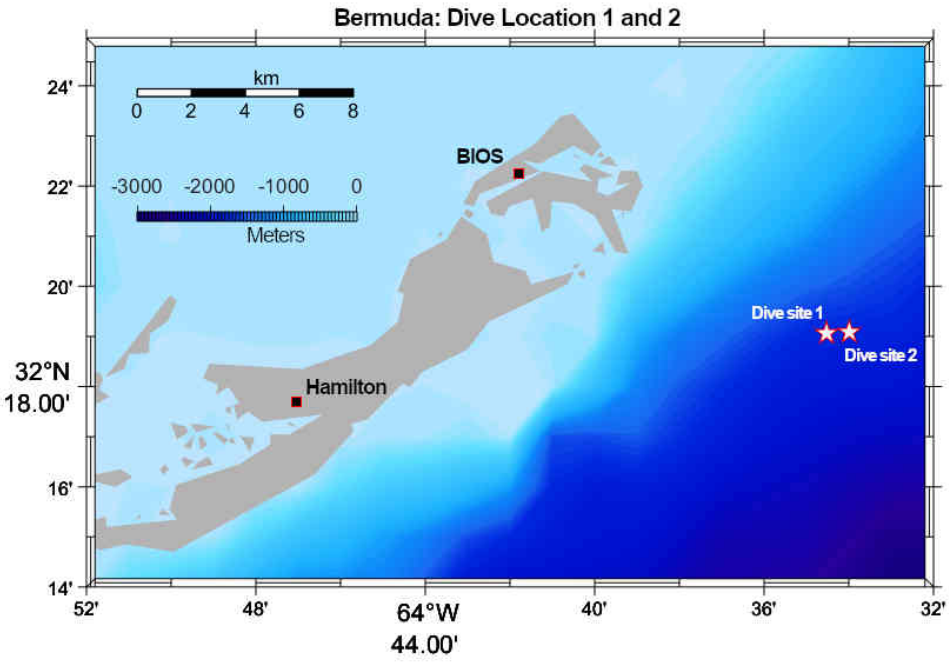

Figure 2: The map shows the dive site in Bermuda where the experiment was conducted. Three dives took place, including a test dive, but only Dive 1 and 2 are marked. This manuscript focuses solely on the datasets collected during Dive 2.

on the water column and its constituents. This approach aims to overcome the limitations of traditional ship-mounted echosounders in observing mesopelagic animals in the deep ocean.

C. ISSUES & LIMITATIONS

Adverse weather conditions were experienced at the dive site, which significantly hindered diving operations and reduced the number of dives conducted. During both data collection dives, technical issues arose with the winch. Specifically, the active-heave compensation mode failed, resulting in strong heave motion of the payload and causing motion blur in the video imagery. Additionally, the ES60 system experienced considerable electrical interference from the winch, despite having isolated power supplies. This interference generated electrical noise that obscured the ES60 echogram during winch operations, requiring the winch to be shut down to effectively observe the SSLs in the water column; the source of the interference was later identified as a common grounding problem. Moreover, one sensor malfunctioned during each dive: the EK80 system in Dive 1 and the video recording system in Dive 2. Consequently, data analysis was limited to Dive 2, where data from both active acoustic systems were available. Post-dive analysis indicated that the 70 and 200 kHz transducers of the EK80 system were affected by electrical noise correlated with light intensity changes. As a result, the analysis of EK80 data was restricted to the 38 kHz transducer, which was unaffected by this issue.

Due to the time constraints and weather, calibration for the EK80 transducers was not carried out. However, calibration for the single-beam ES60 38/200 kHz transducer was performed post-dive utilizing standard sphere calibration techniques for single-beam echosounders.[15,16] It was observed that the returned backscatter values from the 38 kHz EK80 system seem to match very well with the calibrated 38 kHz ES60 system.

3. DATA PROCESSING METHODOLOGY

Figure 3 illustrates the post-dive data processing scheme implemented using custom Matlab scripts. Raw received power was parsed and converted into physical angles, target strength (TS), and volume backscatter (Sv) following the methods outlined in these reports.[17,18] Noise was evident in all echograms, which were caused by multiple sources (see Figure 4 for an illustration of an unfiltered 38 kHz echogram). Subsequently, these data were post-processed using algorithms specifically designed to eliminate noise artifacts due to interference from shared frequencies among transducers (impulse noise), air bubbles (attenuation noise), background noise, and transients caused by the winch.[16,17,19,20] Custom noise removal filters were developed to remove backscatter of the payload observed in the ES60 38 kHz data.

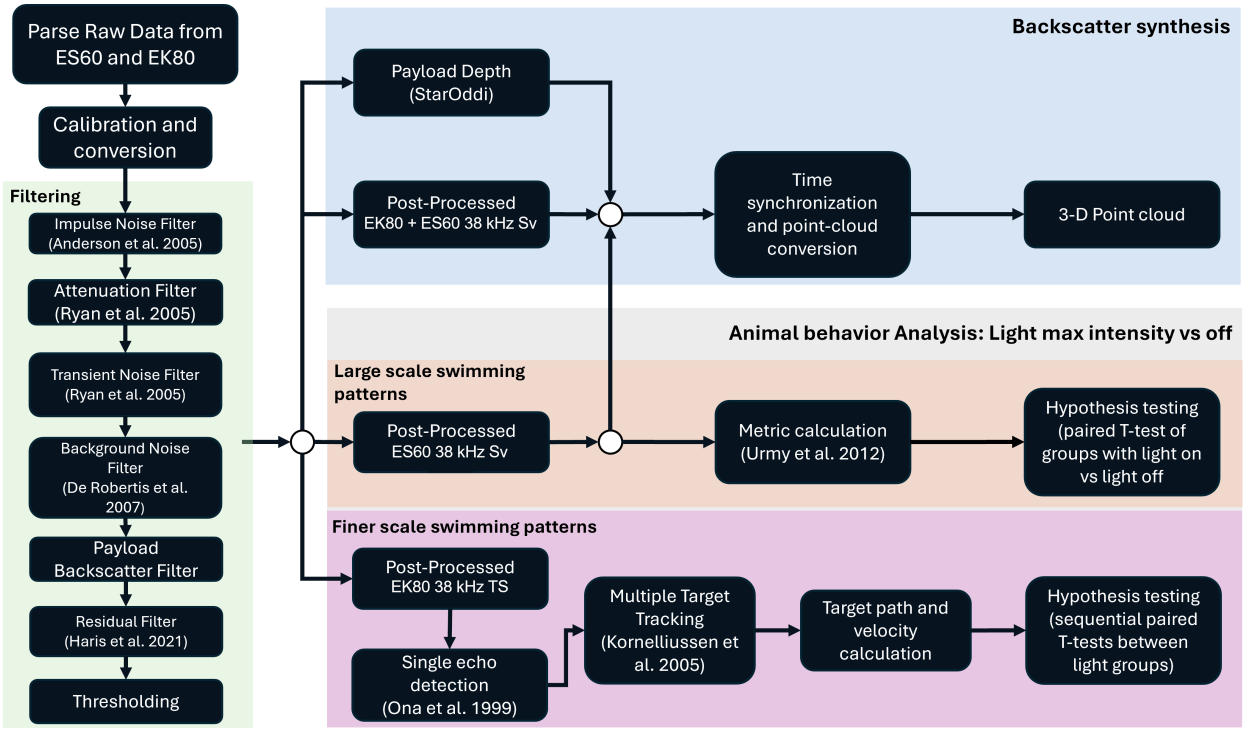

Figure 3: Echosounder data processing scheme from parsing raw received power, post-processing Sv and TS measurements for both the ship-mounted and vehicle-mounted echosounder systems, and synthesizing them together. Data synthesis was performed to combine these measurements, along with data from other instrumentation, to capture backscatter in distinct temporal and spatial scales.

Post-processed Sv data from both systems were time-synchronized and merged into a single 3-D point-cloud map, offering a unique view of animal distribution and migration in the water column. This map provides an illustration of both large- and small-scale backscatter patterns over time, highlighting areas for more detailed analysis. We used two metrics from Urmy et al.[21] to characterize large-scale variations in vertical backscatter data over time and depth during our artificial light experiments, enabling us to observe both temporal and spatial changes that might be associated with the light variation (see Table 1). The first metric, center of mass (COM), indicates how backscatter is distributed across depth, providing insight into animal movements toward or away from the payload. The second metric, inertia, measures the spread of backscatter around the COM, showing whether animals are clustering or spreading out. Together, these metrics may help infer large-scale defensive or foraging behaviors in response to artificial light.

For analyzing smaller-scale swimming patterns of animals in front of the payload over time, we applied single echo detection (SED) based on Ona et al.[22] and multiple target tracking (MTT) based on Handegard

Table 1: Backscatter characterization metrics derived from Urmy et al.,[21] utilized to assess temporal and spatial variations over time and range. Description of parameters: s_v is the linear form of Sv (1/m) and z is water depth (m).

Metric	Notation	Unit	Equation
Center of mass	*COM*	m	$\frac{\int z s_v dz}{\int s_v(z) dz}$
Inertia	*I*	m^{-2}	$\frac{\int (z - COM)^2 s_v(z) dz}{\int s_v(z) dz}$

et al.[23] to the forward-facing split-beam EK80 data. The SED algorithm identifies potential single targets using criterion summarized in Ona et al.,[22] with empirically determined values documented in Table 2. The MTT algorithm then generates possible tracks for these targets, with criteria summarized in Handegard et al.[23] and values determined empirically shown in Table 3. The MTT algorithm generates 4-D swimming trajectories, which we simplify to 3-D by deriving velocity (m/s) of the detected single targets. Finally, hypothesis testing was performed on the derived metrics from the 38 kHz ES60 data and the single-target velocity data from the 38 kHz EK80 to evaluate whether artificial light influenced faunal activity and their aggregations over time.

Table 2: User defined parameters for the SED Algorithm used in this study.

Parameter	Units	Value
TS Threshold	dB ref $1m^2$	-70 to 0
PLDL	dB ref $1m^2$	6
Minimum normalized pulse length	-	0.7
Maximum normalized pulse length	-	1.5
Maximum beam compensation	dB ref $1m^2$	7
Standard deviation of physical angle	degrees	2

4. RESULTS

A. DIVE OVERVIEW FROM THE ES60 DOWNWARD FACING ECHOSOUNDER

Figure 4 presents a graphical overview of what was seen in the ES60 38 kHz system during operations in Dive 2, along with detailed explanations of the events that occurred during this dive. The ES60 echogram was not post-processed to accurately represent primary field observations.

- **Event A**. The winch was activated and deactivated multiple times to locate a target layer for observa-

Table 3: User specified variables for the MTT algorithm used in this study.

Function	Parameter	Units	Value
EKF	Alpha	-	0.7
	Beta	-	0.5
Gating	Exclude distance	m	1
	Standard deviation angle	degrees	1
	Missed ping	percentage	5
Track allocation	Weight alongship angle	percentage	20
	Weight athwartship angle	percentage	20
	Weight range	percentage	40
	Weight TS	percentage	20
	Weight ping gap	percentage	0
Track review	Minimum single targets	-	3
	Minimum pings	-	3
	Maximum ping gap in track	-	3
	Maximum delta TS	-	30

tion. The payload was deployed to a SSL at 30 m. A layer was seen at ∼200 m.

- **Event B**. The payload descended to 200 m. However, upon reaching this layer, the SSL disappeared and was observed at a deeper depth of 270 m.
- **Event C**. The payload was then raised back to 30 m, where numerous animals were observed in the video footage. During this time, Niskin bottle samples for a different collaborative project were collected and the payload was not moved during this period. During the Niskin sampling period (0:26:00 – 0:36:11 UTC), it was noted that a strong aggregation at 270 m began ascending to ∼140 m, exhibiting considerable backscatter strength as observed by the ES60 38 kHz transducer.
- **Event D**. The payload was lowered to observe the layer at ∼110 m and possibly capture the strong upward migrating aggregation. The payload was able to intercept the aggregation. Dive logs reported the likely observation of myctophids in the video stream. The ship engines were turned off at 0:44:37 UTC.
- **Event E**. Another strong migrating layer was seen to ascend from 180 m. This layer halted at 150 m, prompting pursuit. However, upon arrival at 150 m, the layer maintained a consistent vertical distance below the payload, approximately 20 m lower.
- **Event F**. The payload was lowered to the layer at 165 m. However, the ship engine needed to be restarted and minor boat adjustments were made, ultimately resulting in the complete disappearance of the layer by 0:56:51 UTC. Scientists aboard the vessel watching the data streams from the video and acoustic backscatter noted that the activation of the boat engine may have contributed to the disappearance of this layer.
- **Event G**. The payload was lowered to the stable layer at 100 m to conduct light experiments. The experiment was performed by changing light intensity, ranging from off to maximum intensity, at approximately 5-minute intervals. This experiment lasted approximately 30 minutes.
- **Event H**. The final transect was performed at a depth of 35 m, where the layer remained consistently

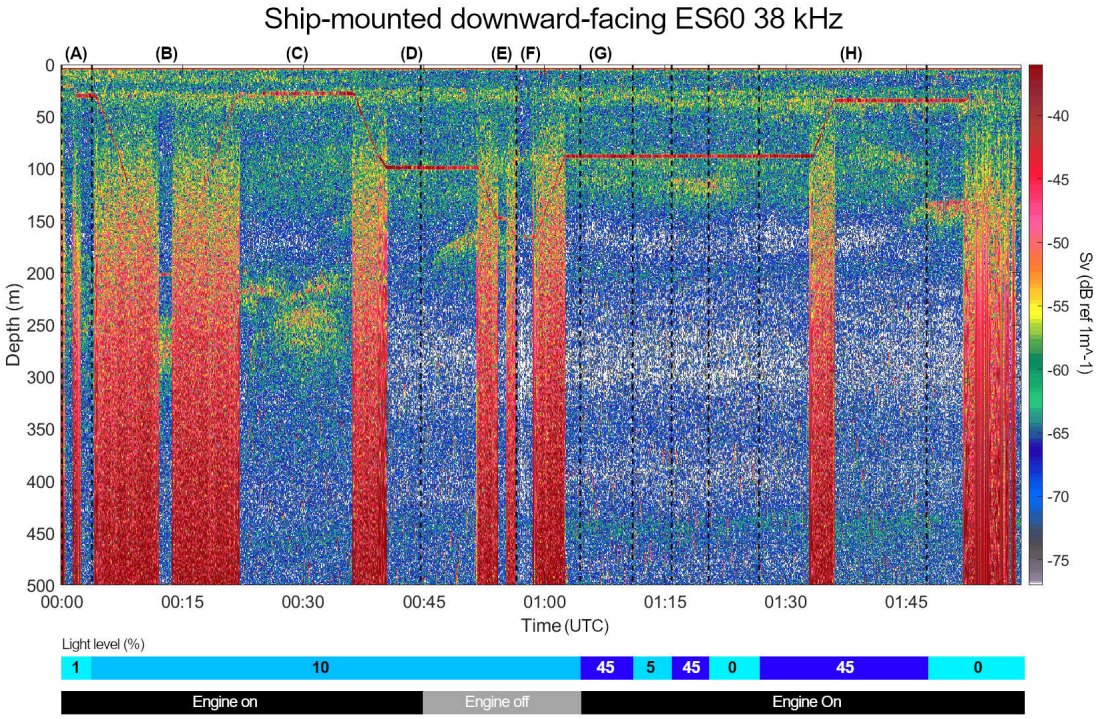

Figure 4: Unfiltered ship-mounted, downward-facing ES60 volume backscatter recorded during Dive 2 post sunset is overlaid with subsea payload light levels and surface vessel engine operation status. The echogram is unfiltered to accurately reflect primary field observations. Letters at the top correspond to events detailed in the text, while vertical black dotted lines mark timestamps of light level changes and engine status. Strong backscatter from the payload (thick red lines) is visible, correlated with CTD depth data. Noise from subsequent winch operations appears as vertical "colorful" artifacts, obscuring animal scattering. Interference from the vehicle-mounted 38 kHz transducer is manifested as red impulses scattered around the echogram.

present throughout the dive. Finally, the payload was recovered at 1:59:22 UTC and the dive ended.

B. ASSIMILATED DOWNWARD AND FORWARD-FACING ECHOSOUNDER DATA

Volume backscatter data from both acoustic systems were post-processed and time-synchronized to create the point-cloud map shown in Figure 5. Snapshots from events (**C**), (**D**), (**E**), and (**F**) documented in the previous section are included. The EK80 system revealed slower-moving organisms during Event (**C**) indicated by the crisp shapes of the sound scatterers (Figure 5(A)). In event (**D**), where the payload intercepted a fast-moving ascending layer, the fused echogram shows a distinct pattern with a sharp gradient of sound scatterers, resembling motion blur in slow shutter speed photography (Figure 5(A)). The disappearance of layers reported in events (**E**) and (**F**) is evident by the voids in the EK80 echogram (Figure 5(B). Light experiments, where intensity was varied over 4 to 6 minutes, were conducted at a SSL located at $\sim$100 m for 30 minutes (Figure 5(C)). During this experiment, the ship-mounted ES60 echogram revealed an aggregation of sound scatterers forming approximately 25 m below the payload (Figure 5(D)).

C. DYNAMIC BACKSCATTER CHANGES DURING LIGHT INTENSITY EXPERIMENTS

Echosounder metrics derived from the ES60 Sv data during light experiments were calculated, and a smoothed trend was obtained using a 10th-degree polynomial regression with a 95% confidence level and a moving average filter (Figure 6). The results showed subtle changes throughout the experiment. Minor

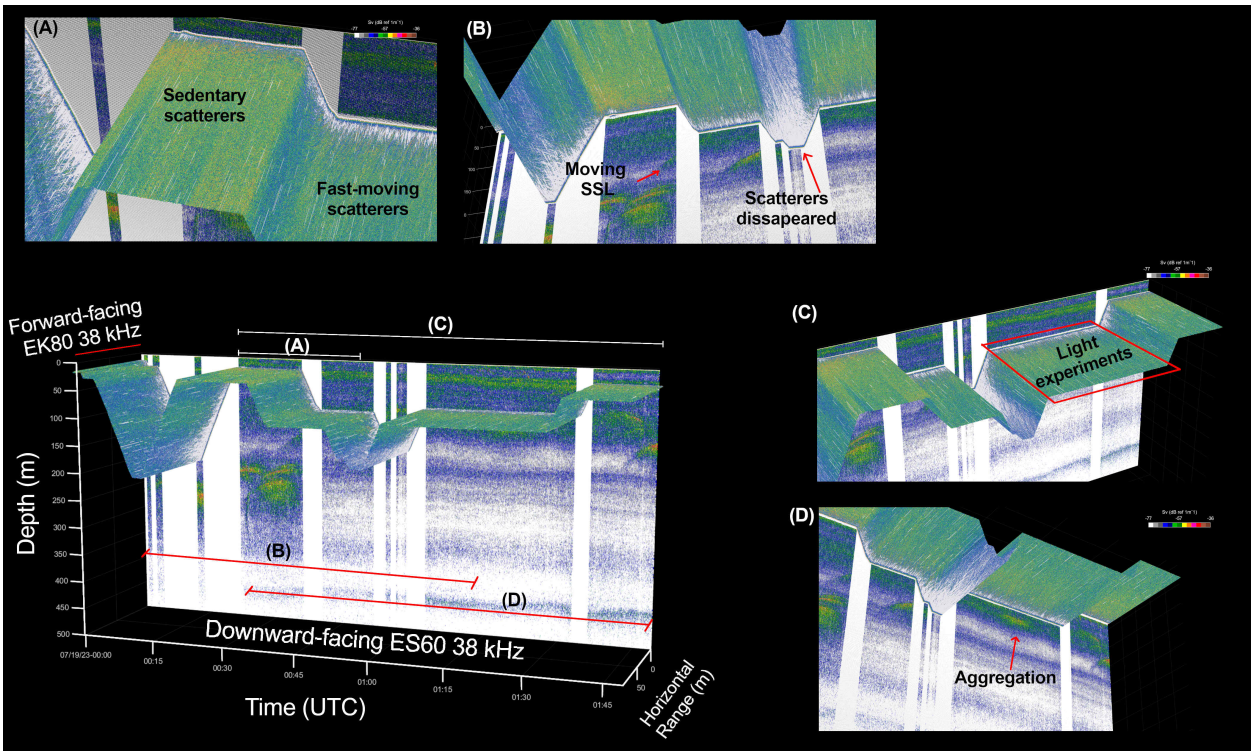

Figure 5: Bottom left panel: An overview of Dive 2 from synchronized post-processed 38 kHz vehicle and ship mounted acoustic systems. The scale of the axis has been adjusted for visualization purposes. (A): Top view illustrating event (C) from Figure 4, where the payload maintained a constant depth at ∼30m during Niskin grabs. This snapshot captured both slow and fast moving scatterers. (B): Bottom view of events (D), (E), and (F). The ascending layer in event (D) (red arrow) coincides with the payload's path. The disappearance of a migrating layer during events (E) and (F) is clearly observed from both echosounder datasets. (C): Top view of event (G) where the payload maintained depth at the SSL located at 100 m and varied light intensity subsequentially with time intervals (red box). (D): Bottom view of event (G) reveals sound scatterers dynamically changing over time and depth during the experiment, where a dense aggregation formed ∼25 m under the payload

fluctuations in the COM metric were observed across each group, with a notable decrease at the end of group 5. The weak upward trend (decrease in COM depth) when lights were off or at low intensity (5%) suggests that the volume backscatter was concentrated closer to the payload depth (∼100 m), while the opposite occurred at maximum light intensity. A decline in Inertia strongly detected the aggregation forming approximately 25 m beneath the payload during light groups 2, 3, and 4. However, paired t-tests between groups subjected to light (1, 3, and 5) and those with low or no light (2 and 4) revealed no significant differences, making it difficult to statistically infer whether the fluctuations in metrics were due to light intensity changes. Additionally, reducing the dimensionality of the volume backscatter data from 3-D to 2-D may limit the ability to detect subtle patterns. Therefore, methods like SED and MTT, which utilize the full dimensions of Sv data, could potentially reveal finer behavior patterns of individual mesopelagic scatterers. These algorithms are particularly applicable to EK80 datasets, as they are suited for shorter ranges and can acquire scattering data in front of the vehicle at midwater depth.

The MTT algorithm identified 14,203 tracks from the 157,389 targets obtained by the SED algorithm. Track lengths ranged from 3 pings (∼2 seconds) to 65 pings (∼40 seconds), with the majority (88.2%) being between 3 and 8 pings long. Notably, 37.45% of the tracks consisted of only 3 pings. The prevalence of these short tracks is likely due to the oscillatory motion of the payload, which caused individual target positions to ”jump” over time, limiting the algorithm's ability to resolve longer tracks. The 3-D target

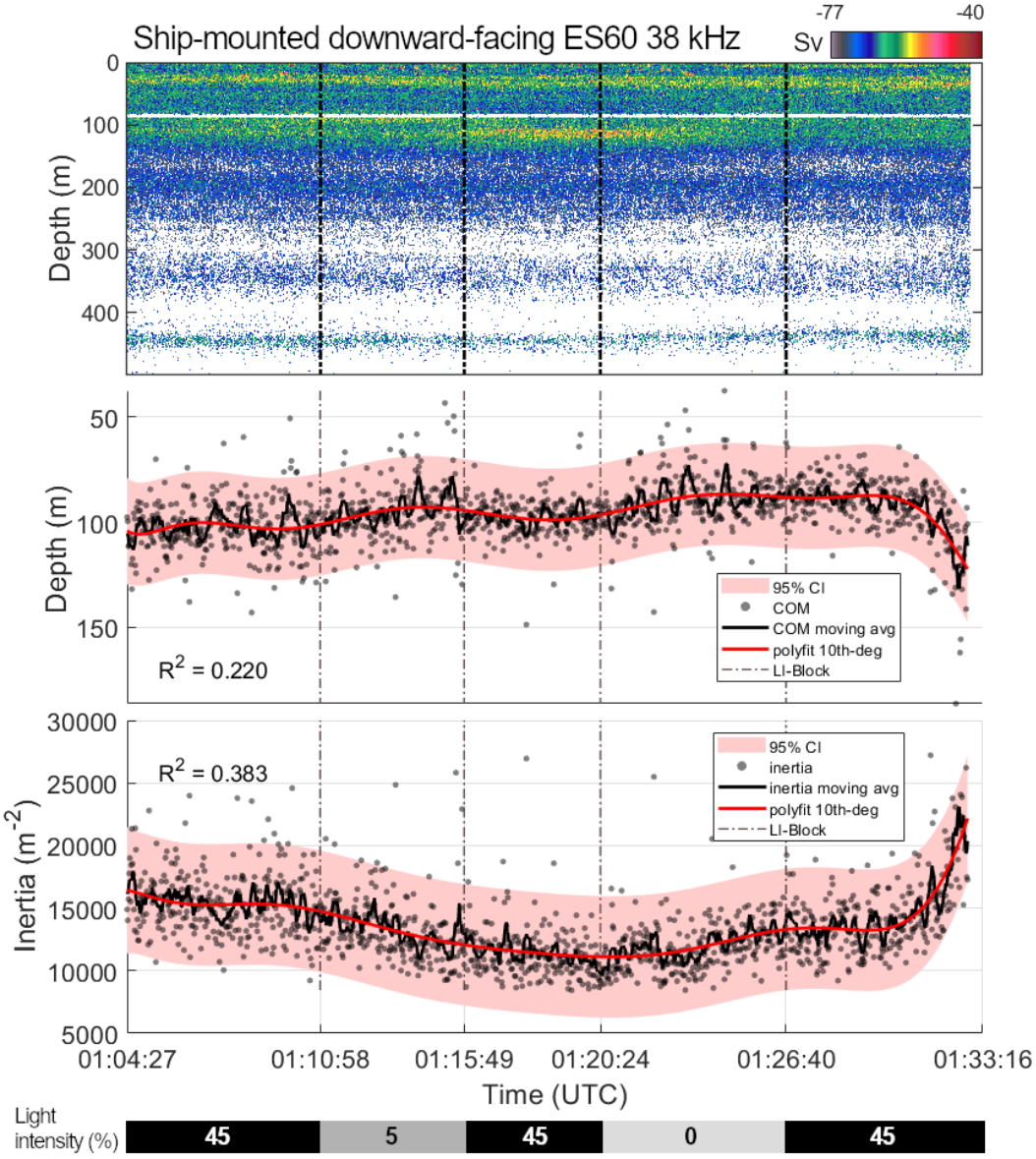

Figure 6: Subset of the downward-facing 38 kHz echogram during light experiments, alongside computed COM and Inertia metrics. Top panel: Post-processed Sv from the ES60 38 kHz channel. Black lines indicate group of pings under different light intensity levels that were varied across ∼5 minutes. Middle panel: Computed COM plotted against time (grey dots) overlaid with the 10-point moving average line (black), 10th-degree polynomial fit line (red), and 95% confidence interval (red area) that represents the computed metric as a smoothed trend. Note the y-axis is flipped to follow the axis (top-panel). Bottom panel: Computed Inertia metric alongside smoothed trend with 95% confidence level. Lower Inertia values suggest higher aggregation of scatterers.

tracks of individual animals were further simplified into velocity (m/s) by applying a gradient to each track. Figure 7(a) illustrates these tracks and their derived velocities, with a color scale indicating negative velocity (blue) for targets swimming towards the payload and positive velocity (red) for those swimming away. The distribution of target velocities, shown as a histogram in Figure 7(b), follows a bell curve, with most velocities between -0.2 and 0.2 m/s. To compare target velocities across different light groups, velocities were grouped based on sequential changes in light intensity and analyzed using two-tailed t-tests. Figure 7(c)

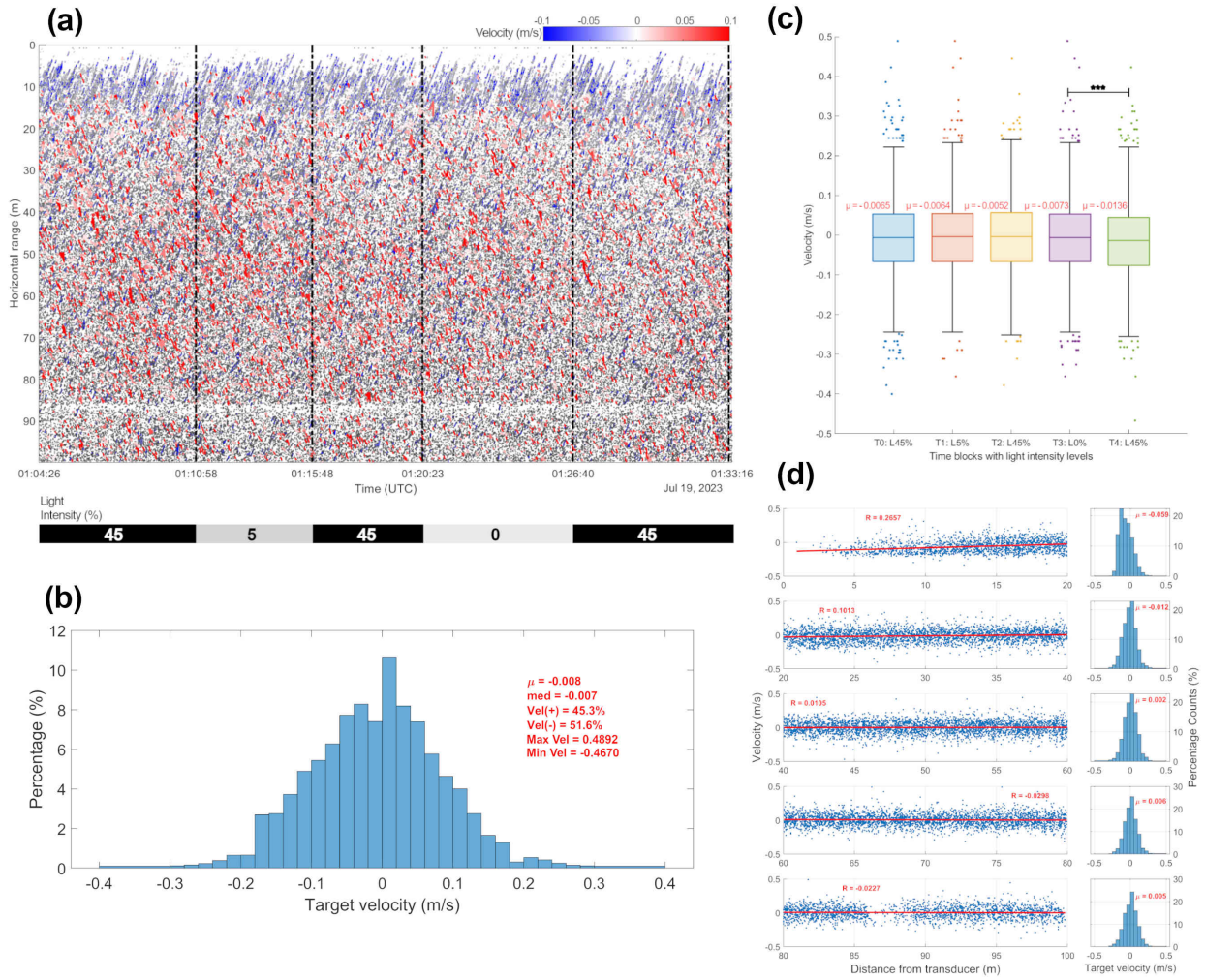

Figure 7: Tracks of targets that are color mapped to the derived velocity (m/s), along with the velocity histogram and box plots, and correlation between velocity and horizontal distance from the payload. (a): Velocity of detected single targets. Positive velocity values (red) suggests animals that were swimming away from system while negative velocity values (blue) suggests otherwise. Vertical black lines are timestamps when light intensity changes were made (bottom of figure). (b): Histogram of the velocity distribution for all single targets. (c): Box plots of velocity distributions for each light intensity group. Outliers are shown above and below each box. Sequential paired t-test with significant results ($p < 0.005$) are marked with (***). (d): Correlation analysis of single target velocity grouped in 20 m range intervals with their underlying distributions. First column is scatter plots of velocity vs distance of targets for different range intervals, overlaid with correlation line and R value. Second column is the distributions and corresponding mean value.

shows box plots indicating a significant difference only between group 4 (no lights) and group 5 (maximum light intensity), with no other significant variations observed among other group pairs. Velocity outliers exceeding 0.4 m/s were consistent in groups 1 to 4, while group 5 had the lowest velocity distributions. These observations suggest that light intensity has no significant effect on the animal's avoidance or attraction behavior.

We hypothesized that fauna closer to the payload might be more affected by the lights. To test this, we grouped the velocities of single targets into 20-meter range bands and analyzed them for correlation. A positive correlation suggests that animals closer to the system would tend to swim towards the system

(attraction), while animals at a larger distance would swim away (avoidance). On the other hand, a negative correlation would indicate the opposite reaction. Figure 7(d) shows the results of this correlation across different distance bands. A weak positive correlation (R = 0.2657) was observed in the 0-20 m distance band, indicating that some animals at a closer distance (<12 m) seem to swim towards the system, while animals above this range seem to swim away. In addition, this particular distance band has a unique left-tailed distribution where most velocities are negative (attraction). No significant correlation (R≈0) was found at other range intervals (>20 m). Due to technical issues with the video recording and the lack of additional biological sampling, we were unable to obtain taxonomic information on the detected scatterers.

5. CONCLUSION

New technological advances could potentially provide new insights on classical problems, such as understanding more about the mesopelagic environment. Investigating the mesopelagic realm remains difficult due to the resource demands on data collection, especially when collected in real-time. Despite numerous technical difficulties, we were able to demonstrate the capability of our mesopelagic observing system to document and track mesopelagic animals in the water column using multiple active acoustic systems and imaging. Only one dive was worthy to process, which gathered data in the 38 kHz channel from all acoustic systems but without video data. We opportunistically conducted a field experiment to observe changes of light intensity towards animal behavior and found no statistical significance from both acoustic systems when lights were alternated on and off. However, the forward-facing echosounder was able to tease out a weak positive correlation of velocity vs distance of animals within 20-meters of the system. This suggests that animals may swim towards or away from the system depending on their relative distance, irrespective of artificial light levels. Further investigation is needed, and a comprehensive survey design should be developed to allow for species identification, either through traditional biological sampling or broadband acoustics. Interestingly, an unidentified migrating SSL appeared to avoid the system during both dives, suggesting these organisms may detect the system despite its minimal environmental impact, raising important questions for future research.

ACKNOWLEDGMENTS

The data collection described would not be possible without the invaluable support and local knowledge of Chris Flook and Kyla Smith at the Bermuda Institute for Ocean Sciences. We would also like to thank Jason Noel, Alexander Yin, Breanna Motsenbocker, and Brian Leong for their field work assistance. This work was supported by Office of Naval Research Task Force Ocean Grant 13634725.

REFERENCES

[1] A. W. Stoner, C. H. Ryer, S. J. Parker, P. J. Auster, and W. W. Wakefield, "Evaluating the role of fish behavior in surveys conducted with underwater vehicles," *Canadian Journal of Fisheries and Aquatic Sciences*, vol. 65, pp. 1230–1243, June 2008.

[2] K. J. Benoit-Bird, C. M. Waluk, E. J. Martin, K. R. Reisenbichler, R. E. Sherlock, P. R. McGill, and B. H. Robison, "Schrödinger's fish: Examining the robotic observer effect on pelagic animals," *Limnology and Oceanography: Methods*, vol. 21, no. 9, pp. 563–580, 2023. Publisher: Wiley Online Library.

[3] E. J. Warrant and N. A. Locket, "Vision in the deep sea," *Biological Reviews*, vol. 79, pp. 671–712, Aug. 2004.

[4] S. Kaartvedt, A. Røstad, A. Opdal, and D. Aksnes, "Herding mesopelagic fish by light," *Marine Ecology Progress Series*, vol. 625, pp. 225–231, Aug. 2019.

[5] M. Peña, J. Cabrera-Gámez, and A. C. Domínguez-Brito, "Multi-frequency and light-avoiding characteristics of deep acoustic layers in the North Atlantic," *Marine Environmental Research*, vol. 154, p. 104842, Feb. 2020.

[6] M. J. Underwood, A. C. Utne Palm, J. T. Øvredal, and Bjordal, "The response of mesopelagic organisms to artificial lights," *Aquaculture and Fisheries*, vol. 6, pp. 519–529, Sept. 2021.

[7] M. Geoffroy, T. Langbehn, P. Priou, Varpe, G. Johnsen, A. Le Bris, J. A. D. Fisher, M. Daase, D. McKee, J. Cohen, and J. Berge, "Pelagic organisms avoid white, blue, and red artificial light from scientific instruments," *Scientific Reports*, vol. 11, p. 14941, July 2021.

[8] E. Widder, B. Robison, K. Reisenbichler, and S. Haddock, "Using red light for in situ observations of deep-sea fishes," *Deep Sea Research Part I: Oceanographic Research Papers*, vol. 52, pp. 2077–2085, Nov. 2005.

[9] R. Mitson, "Causes and effects of underwater noise on fish abundance estimation," *Aquatic Living Resources*, vol. 16, pp. 255–263, July 2003.

[10] A. De Robertis and N. O. Handegard, "Fish avoidance of research vessels and the efficacy of noise-reduced vessels: a review," *ICES Journal of Marine Science*, vol. 70, pp. 34–45, Jan. 2013.

[11] M. Peña, "Mesopelagic fish avoidance from the vessel dynamic positioning system," *ICES Journal of Marine Science*, vol. 76, pp. 734–742, May 2019.

[12] D. F. Gruber, B. T. Phillips, L. Marsh, and J. S. Sparks, "In situ Observations of the Meso-Bathypelagic Scyphozoan, *Deepstaria enigmatica* (Semaeostomeae: Ulmaridae)," *American Museum Novitates*, vol. 3900, pp. 1–14, May 2018.

[13] C. Roman, D. S. Ullman, D. Hebert, and S. Licht, "The Wire Flyer Towed Profiling System," *Journal of Atmospheric and Oceanic Technology*, vol. 36, pp. 161–182, Feb. 2019.

[14] B. Grassian, C. Roman, J. D. Warren, and D. Casagrande, "High-resolution measurements of the epipelagic and mesopelagic ocean by a profiling vehicle equipped with environmental sensors and a broadband echosounder," *Limnology and Oceanography: Methods*, vol. 21, pp. 106–125, Feb. 2023.

[15] J. Warren, T. K. Stanton, M. C. Benfield, P. H. Wiebe, D. Chu, and M. Sutor, "In situ measurements of acoustic target strengths of gas-bearing siphonophores," *ICES Journal of Marine Science*, vol. 58, pp. 740–749, Aug. 2001.

[16] D. A. Demer, L. Berger, Bernasconi, Bethke, K. M. Boswell, D. Chu, Domokos, A. J. Dunford, Fässler, S. Gauthier, L. C. Hufnagle, J. M. Jech, N. Bouffant, Lebourges-Dhaussy, Lurton, G. J. Macaulay, Y. Perrot, T. E. Ryan, Parker-Stetter, Stienessen, Weber, and Williamson, "Calibration of acoustic instruments," Tech. Rep. NO. 326, International Council for the Exploration of the Sea, 2015.

[17] L. N. Andersen, D. Chu, N. O. Handegard, H. Heimvoll, R. Korneliussen, G. J. Macaulay, E. Ona, R. Patel, and G. Pedersen, "Quantitative processing of broadband data as implemented in a scientific split-beam echosounder," *Methods in Ecology and Evolution*, vol. 15, pp. 317–328, Feb. 2024.

[18] K. Maritime, "EK80 Wide band scientific echo sounder Interface specifications," Interface specifications Release 23.6.0, Kongsberg Maritime AS, Aug. 2023.

[19] T. E. Ryan, R. A. Downie, R. J. Kloser, and G. Keith, "Reducing bias due to noise and attenuation in open-ocean echo integration data," *ICES Journal of Marine Science*, vol. 72, pp. 2482–2493, Oct. 2015.

[20] K. Haris, R. J. Kloser, T. E. Ryan, R. A. Downie, G. Keith, and A. W. Nau, "Sounding out life in the deep using acoustic data from ships of opportunity," *Scientific Data*, vol. 8, p. 23, Jan. 2021.

[21] S. S. Urmy, J. K. Horne, and D. H. Barbee, "Measuring the vertical distributional variability of pelagic fauna in Monterey Bay," *ICES Journal of Marine Science*, vol. 69, pp. 184–196, Mar. 2012.

[22] Ona, E., Barange, Kloser, Miller, Everson, Reynisson, Holliday, Rudstam, and Traynor, "Methodology for Target Strength Measurements (With special reference to in situ techniques for fish and mikro-nekton)," ICES Cooperative Research Report No. 235 No. 235, International Council for the Exploration of the Sea, 1999.

[23] N. O. Handegard and D. Tjøstheim, "When fish meet a trawling vessel: examining the behaviour of gadoids using a free-floating buoy and acoustic split-beam tracking," *Canadian Journal of Fisheries and Aquatic Sciences*, vol. 62, pp. 2409–2422, Oct. 2005.